ATU
PRESS

Original Research

The Effect of Architectural Design Parameters on IEQ in School Smartification

Sahar Mohammadi [iD]	PhD Candidate, Faculty of Architecture and Urbanism, Imam Khomeini International University, Qazvin, Iran
Yousef Gorji Mahlabani *[iD]	Professor, Department of Architecture, Faculty of Architecture and Urbanism, Imam Khomeini International University, Qazvin, Iran.
Fariborz Karimi [iD]	Assistant Professor, Department of Architecture, Faculty of Architecture and Urbanism, Imam Khomeini International University, Qazvin, Iran.
Babak Mohammad Hoseini [iD]	Assistant Professor, Department of Physics, Faculty of Science, Imam Khomeini International University, Qazvin, Iran.

Abstract

Purpose: The study aims to study the effect of architectural design parameters on IEQ in accomplishing school smartification.

Method: The research was conducted in school buildings located in Tabriz, Iran. The indicators chosen to represent IEQ are the adaptive PMV model used for thermal comfort, imageless daylight glare probability used for visual comfort, and CO_2 concentration used for

IAQ assessment. The simulation technique was used to collect data for a generative parametric school model. The method of data analysis includes a multivariate linear regression algorithm, t-test statistic, and one-way analysis of variance. The studied variables are dimensions of classrooms with the fixed area, Percentage of window area on a wall, window height, Shading, and protrusions in plan design. The stepwise method for multivariate linear regression in SPSS was used to assess the vital IEQ indicator in terms of thermal and visual comfort and CO2 concentration.

Findings: The study found that among studied indicators, the south facade window ratio significantly correlates with IEQ. The other parameters are the north window ratio and north window height. the findings revealed that to increase the IEQ in schools, facade design is more critical than the plan. The higher the window surface on the south, north, west, and east faces, the greater the thermal comfort and glare probability is.

Conclusion: However, increasing the height of the windows can reduce glare and also increase thermal comfort. Thermal comfort improves as the length of the southern classrooms rises. On the bright side, it has no noticeable glare effect.

Keywords: IEQ, Thermal comfort, Visual comfort, IAQ, Optimization, Smart schools.

1. Introduction

According to recent studies, interior environment quality (IEQ) has a direct association with the health and efficiency of people in the workplace and educational environments (Fisk, 2000, 2002; Fisk, Black, & Brunner, 2011).

Schools are becoming smart places as a result of technological advancements and the rising trend of building intelligence (Renz & Hilbig, 2020). School smartening is a type of preparation for an educational center's demands that boosts pupils' positivity and

intelligence. School intelligence has become so widespread around the world that school administrators are considering its quality and kind (Mogas, Palau, Fuentes, & Cebrián, 2021). Thermal, visual, and acoustic comfort and indoor air quality are the factors that influence the IEQ index (Diaz, Piderit, & Attia, 2021; W. Wei, Wargocki, Zirngibl, Bendžalová, & Mandin, 2020). Energy consumption is necessary to provide cooling, heating, lighting, and ventilation to the degree that they are required for human comfort (Asadi, Mahyuddin, & Shafigh, 2017; Pereira, Lamas, & da Silva, 2019). As a result, the two measures of building energy use and indoor air quality are linked. Developing the concepts and methods of architectural design in such a way as to decrease energy consumption in the building demands a strategic approach. Schools, where students spend the majority of their time, are one of the most significant structures whose architecture influences the quality of learning (Catalina & Iordache, 2012). The quality of the interior environment can be assessed and questioned objectively in the built structures, or by analyzing design criteria used to compute or simulate yearly energy performance for buildings under construction (Kabele, Veverková, & Urban, 2019; Karapetsis & Alexandri, 2016). Smart schools are still an exploratory field of research and innovation. Specific intelligent services, such as ICT, content delivery devices and tools, approaches for improving student involvement, automatic review of student contributions, and student attendance management, are the most common developments (Saini & Goel, 2019). The comfort of a building is heavily influenced by architectural design aspects. Numerous studies have been conducted on the link between form parameters and the scale of a single building (Alghamdi, Tang, Kanjanabootra, & Alterman, 2022; Lang, Wargocki, & Liu, 2022; L. Wei et al., 2016). Building typology, orientation, building form, building shell, interior design, and complementing components are the six categories of architectural design considerations. Figure 1 depicts the subsets of each group. Several factors have an impact on the building's internal atmosphere (Zhang et al., 2022). One essential choice, for example, is the size of the windows, which can diminish or raise the inside comfort conditions (visual, acoustic, thermal) (Bahaj, James, & Jentsch, 2008). Knowing the proper quantity throughout the design process, on the other hand, is more valuable than analyzing its usefulness after the

occurrence. In architectural decision-making challenges (Rahbar, Mahdavinejad, Markazi, & Bemanian, 2022), parametric models and optimization tools are effective solutions to attain the required goals (Hollberg & Ruth, 2016; Holzer, Hough, & Burry, 2007; Razmi, Rahbar, & Bemanian, 2022). The school building is defined as a parametric model in this article, which then assesses the effect of modifying design parameters on thermal and visual comfort, as well as interior air quality, using simulation tools in the Grasshopper plugin. The simulation approach is used to examine the efficiency of the interior environment throughout the design process. By identifying these elements, an effective initial step in recognizing strategies to increase student participation to improve the IEQ and the school's smartification will be taken.

Figure 1 Architecture design factors
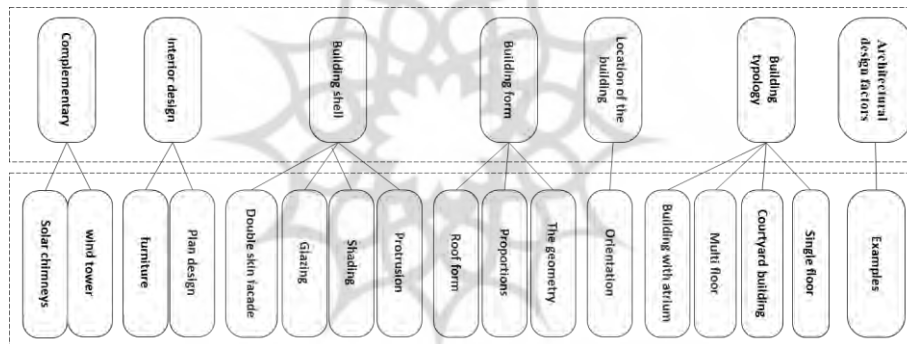
2. Method

The study begins with an examination of the features of Tabriz school plans and facades, as shown in Figure 2. The results regarding the different dimensions and sizes of the classrooms, the number of floors, and the arrangement of the spaces have been investigated by comparing and analyzing the technical documents of the sample schools. A parametric model has been designed based on the dominant sample of schools. Automated modeling, simulation, and assessment approaches implemented in Grasshopper software are used to collect data in this study. The following are some of the plugins and simulation engines that are used in this process: Grasshopper is in

charge of the parametric modeling of a school building in the first stage, which will be responsible for the sampling. The parametric design was used to create a mix of characteristics such as class dimension, percentage of openings, and canopy size. In the second section, the Ladybug and Honeybee plugins will use the Energy Plus and Open Studio engines to evaluate building performance in terms of thermal comfort and carbon dioxide concentration. Glare analysis is also done using the radiance engine (Figure 3). This step is done 250 times using an automated cycle to update the design parameters and save the simulation results in the program. Alternatively, 250 examples of various designs were tested for thermal comfort, visual comfort, and indoor air quality. To study the link between the researched parameters and selected indicators, the gathered findings and data of the samples collected in Grasshopper software were analyzed using multivariate linear regression in a stepwise method in SPSS.
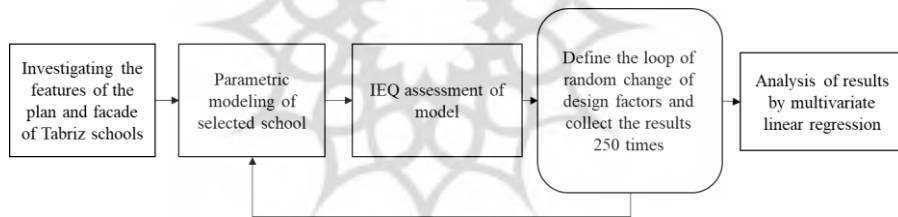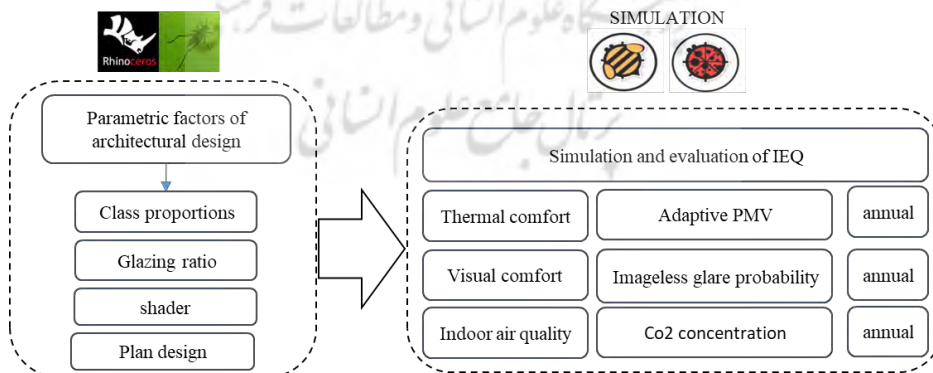

Figure 2. Research methodology

Figure 3. Modeling and simulation details

2.1. Productive design

To create a parametric school model, seventy samples of Tabriz schools were investigated. The following was generally true of their plan: 1. The classrooms were arranged in a hedge, with the communication area in the middle of the two rows of classrooms. 2. the interface is positioned on the length axis; however, if there are other entries, they are placed close to the width axes. 3. The majority of the staircases are in the length and width axes, in front of the entryway. 4. Patio usage is uncommon. 5. The entrance's maximal direction is south. Schools have a rectangular and longitudinal plan with a width of thirteen to twenty-eight meters and a length of fifteen to seventy meters. The most common ratio of length to width is two to one, with a width of sixteen meters and a length of thirty meters. The rectangular shape with no more fractures has been utilized in the plans. A tiny percentage had depressions and protrusions in relation to the plan's primary rectangle. Figure 4 shows the types of fractures and their frequency.
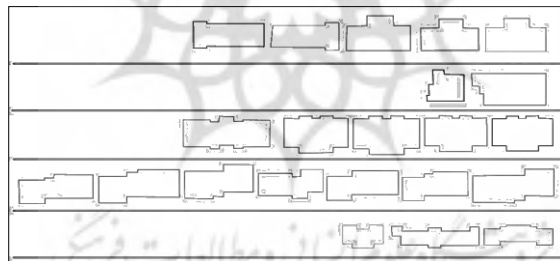

Figure 4 The examined school's plan

According to Table 1, two-story structures without basements represent around 40% of the samples in terms of floor count. In general, the findings revealed that the hallway is regarded as the major area in the plans, with classrooms and other spaces placed around it.

Table 1. Frequency of surveyed schools in terms of number of floors

| 4.22% | 43.66% | 16.90% | 26.76% | 7.04% | **1.4%** |
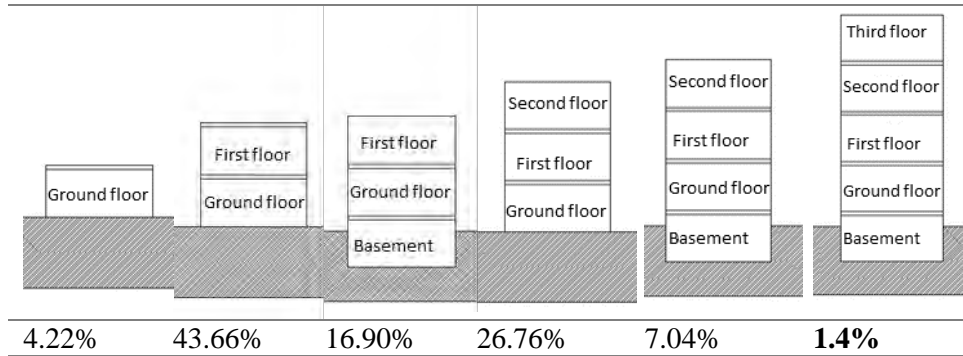
As a result, the chosen model for parametric design is developed in the manner shown in Figure 5. The influence of building orientation (Buratti, Moretti, Belloni, & Cotana, 2013; Mazzeo & Kontoleon, 2020), type of material (Latha, Darshana, & Venugopal, 2015), opening rate (Lyons, Arasteh, & Huizenga, 2000; Singh, Garg, & Jha, 2008), space dimensions, type of canopy (Middel, Selover, Hagen, & Chhetri, 2016), and size on thermal comfort has been shown in studies. The size of windows and canopies is also appropriate in terms of visual comfort (Lee & Tavil, 2007; Tzempelikos & Chan, 2016).

The following variables were chosen for examination in this study, with the rest of the components remaining constant. The variables of classroom length with the fixed area, the proportion of window area to the wall, canopy size, and ledge in the plan, which are stated in Table 2, were chosen for this study.

Table 1. Parametric design variables

no	Design variables	Range	Design feature scope
		Min Max	
V.1	Length of class no. 1	5.00 to 8.00	Shape
V.2	Length of class no. 2	5.00 to 8.00	Shape
V.3	Length of class no. 3	5.00 to 8.00	Shape
V.4	Length of class no. 4	5.00 to 8.0	Shape
V.5	Length of class no. 5	5.00 to 8.00	Shape
V.6	Length of class no. 6	5.00 to 8.00	Shape
V.7	South and west window height	1.0-2.0m	Fenestration
V.8	North and east window height	1.0-2.0m	Fenestration
V.9	Window ratio on south	0-0.9%	Fenestration

V.10	Window ratio on east	0.2-0.9%	Fenestration
V.11	Window ratio on north	0-0.9%	Fenestration
V.12	Window ratio on west	0.2-0.9%	Fenestration
V.13	Depth of shader	0-0.9%	Shading

A numerical interval governs the design variables, which are all part of the architectural geometry. A corridor is constructed in the center of the plan based on the selected sample. Corridors and staircases, as well as places other than the classroom, were deemed fixed in the parametric model. The length-to-width ratio of classes will vary. Their area and location in the plan are regarded as fixed.
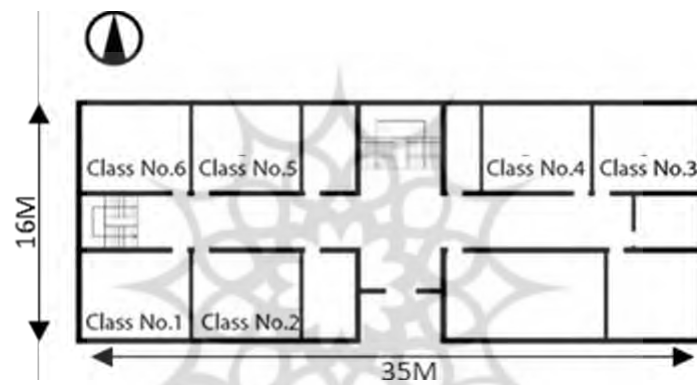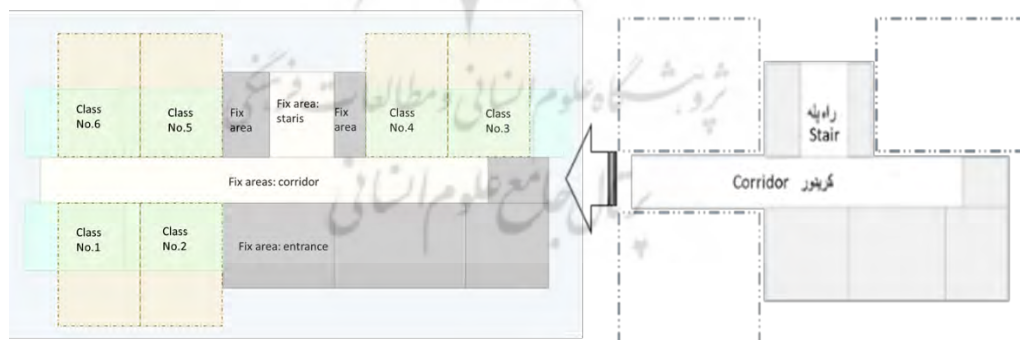

Figure 4. Selected school model

Figure 5. Description of changing the dimensions of classes

The length of each class is chosen between five and eight meters. Each class has a length of between five and eight meters. The width of the class is computed automatically by dividing the 42 (area of the

classes) over the given length. The second story is laid out equally to the first one. Figure 6 demonstrates how the size of classes in a parametric model is adjusted. The windows are designed as a proportion of the façade, and each side of the facade has a slider (north, south, east, west). The range was chosen between 0.2 and 0.9 for the northern and southern faces. Because windowless classrooms appear at zero intervals. there was no requirement for east and west windows so the design procedure allowed for their removal, east, and west windows ranged from 0 to 0.9. The canopy's depth, which is solely designed for south windows, ranged from 10 to 90 cm. A conditional method was created for the beginning height of the windows in such a manner that if the area of the windows is greater than or equal to 40% of the facade surface, its value is 90 cm, and if it is less than 40%, its value is 1 meter and 10 cm. Following the modeling procedure, the masses were transformed into a thermal zone, and the high school's physical program was changed using a plug-in tool. Each building zone has a specific function allocated to it. The wall, window, ceiling, and floor structural parameters are based on the features of typical Iranian construction, as shown in Table 3.

In its models, this study employed Tabriz city climatic data. The winters are frigid, while the summers are sweltering. Its climate may be described as arid and chilly. The meteorological file utilized in this study is for Tabriz Airport, which is located at an altitude of 1367 meters and has a latitude of 38.05 North and a longitude of 46.27 East ("energy plus weather data," 2021).

Table 2. Details of simulated materials

R-Value (m2 - ∘K]/W)	Specific Ht (kJ/[kg - ∘K)	Density (kg/m3)	thickness (MM)	Layers
Exterior Wall layers details				
0.054	1.09	800	15	gypsum plaster
0.39	0.840	1300	150	Clay block
1.04	0.836	265	50	Wall insulation
0.39	0.840	1300	100	Clay block
0.30	0.840	1700	30	Facade brick

R : 1.178 m2.K/W :		U :0.848W/m2.K		
Interior Wall layers details				
0.054	1.09	800	15	gypsum plaster
0.39	0.840	1300	150	Clay block
0.054	1.09	800	15	gypsum plaster
R : 0.8869 m2.K/W		U :11.274W/m2.K		
Window material				
Visible transmittance		Solar heat gain coefficient		U-value (W/m2.K)
0.76		0.45		1.8

2.2. Simulation

In this work, the adaptive PMV model was used as a thermal comfort indicator. According to ASHRAE 55 (Handbook-Fundamentals & Edition, 2009), it is a model that manages the internal temperature or allowed temperature range using outer climatic or metrological elements and is determined based on climatic conditions outside the structure. According to a significant number of studies (Choudhury, Majumdar, & Datta, 2011), human well-being is determined not only by physiology and heat transmission mechanisms but also by social factors and psychological responses to the environment. Honeybee calculated the adaptive thermal comfort coefficient, which was utilized to estimate the degree of thermal discomfort, using the Open Studio engine (Figure 7).
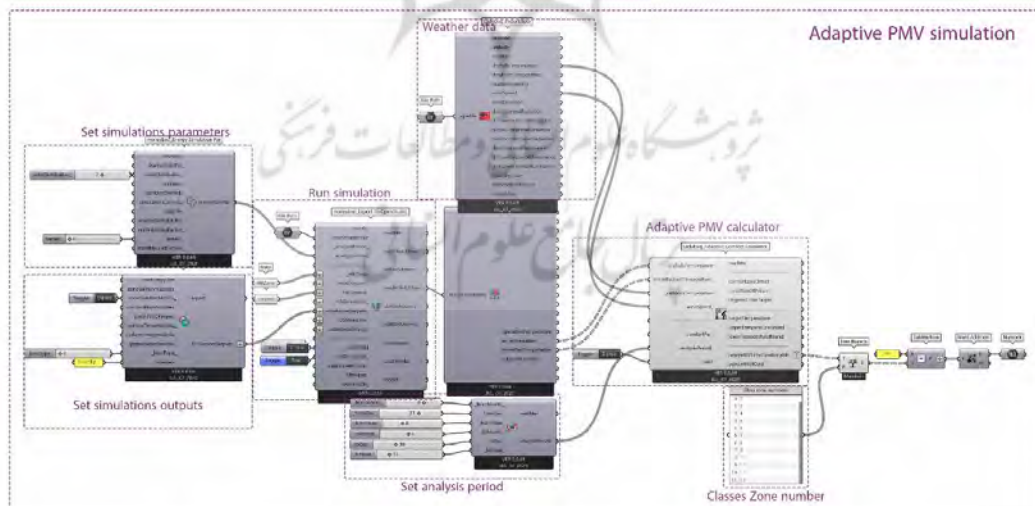

Figure 6. Simulation process of thermal discomfort in Grasshopper software

The Daylight glare probability (DGP) is a visual comfort performance indicator (Chaloeytoy, Ichinose, & Chien, 2020). Wienold and Christoffersen (Wienold & Christoffersen, 2005) proposed this short-term, local, single-domain index to quantify glare. In 2006, it was authorized (Wienold & Christoffersen, 2006). The crucial thing to remember about daylight glare is that, while it was created to explore glare in recorded photographs, it can still be used to assess glare in simulated images. As a result, it is the most acceptable criterion for assessing glare difficulties, according to Sook and Schiller (Suk, Schiler, & Kensek, 2013). The drawback is that it takes longer than many other indications that only require basic analytical computations. First, the designer must select one or more favorite positions that are relevant to the initial occupants of the space. Radiation image format renderings should be provided and finally, the light radiation evaluation performed using Evalglare software, advanced software that can detect light sources in 180-degree ocular scene. Wienold (Wienold, 2007) also provides a simpler form in which, depending on the local values, the logarithmic expression is omitted (brightness and solid angle of the source viewed from the point of view). Nathaniel Jones (Jones, 2019) proposed a method for calculating annual light output in less time without the requirement for picture rendering to solve the problem. The approach used to examine glare in this article is the potential of glare without a picture (Figure 8). The phrase "carbon dioxide concentration" is commonly used to describe the quality of indoor air in terms of the amount of ventilation necessary to lower the concentration of contaminants (Wargocki, Wyon, Sundell, Clausen, & Fanger, 2000). This indicator is appropriate for ventilation (Kapalo, Vilcekova, & Voznyak, 2014), and the link between it and indoor air quality has been thoroughly established. Internal quality standards such as ASHRAE (Handbook-Fundamentals & Edition, 2009) and EN15251 (Comite'Europe'en de Normalisation, 2007) provide minimum

ventilation rate criteria. Carbon dioxide concentrations exceeding 1000 ppm, according to research (Cetin, 2016), can harm inhabitants' health.

Figure 7. Visual comfort simulation workflow in Grasshopper software

The Energy Plus motor is utilized in this model to assess this factor. Energy Plus is one of the most extensively used energy modeling tools, capable of calculating carbon dioxide concentration (based on occupation production, and decrease related to external air infiltration (Figure 9).

Figure 8. CO2 concentration simulation workflow in Grasshopper software

3. Results

If the linear correlation is selected, the coefficient may be obtained from the database using multivariate linear regression. The relationship between the investigated factor, in this case, thermal discomfort, visual discomfort, and carbon dioxide concentrations exceeding 800 ppm were expressed as the following equation utilizing the 13 components listed in Table 2.

(1)

$$Y = b_0 + b_1x_1 + b_2x_2 + b_3x_3 + b_4x_4 + b_5x_5 + b_6x_6 + b_7x_7 + b_8x_8 + b_9x_9 + b_{10}x_{10} + b_{11}x_{11} + b_{12}x_{12} + b_{13}x_{13} + e$$

Where x1, x2,... x13 represent each of the 13 factors studied, and y represents lack of thermal comfort, glare probability, and carbon dioxide concentration, respectively, and b0, b1, b13 represent correlation coefficients, and e represents an error due to the removal of external factors from the model. To define the values b0, b1… b13 and the subsequent weighting scheme, a multivariate linear regression algorithm can be used to obtain the values of the coefficients in the database extracted from the simulation.

The first regression is related to determining the coefficients of thermal discomfort. According to Table 4, the first variable to enter the stepwise multivariate regression equation was the percentage of the south window ratio, which has a correlation coefficient of 0.969 and a significant level of 0.000. These positive numbers imply that these two variables have a meaningful association. The modified coefficient also shows that the ratio of the area of the south window to the wall is responsible for 93.8 percent of the thermal discomfort.

Other variables, such as class 1 length, west window percentage, north window percentage, class 2 length, east window percentage, class 5 length, and class 6 length, have a smaller influence in comparison to this component, as do other factors linked to coefficients. Correlations of less than 0.05 are ignored in the model and do no influence on thermal discomfort. The lengths of classes 5 and 6 in the T-test have a low number and a significance level of higher than 0.00 among the variables submitted. As a result, they do

no influence on the model, and Model 6 is the best equation for predicting thermal discomfort among the analyzed variables across the eight models provided.

Table 3. Details of stepwise regression models for thermal discomfort based on SPSS

model	Variables entered into the thermal discomfort equation	method
1	Window ratio on south	
2	Length of class no. 1	
3	Window ratio on west	
4	Window ratio on north	Stepwise
5	Length of class no. 2	
6	Window ratio on east	
7	Length of class no. 5	
8	Length of class no. 6	

Table 4. Details of the introduced regression models of thermal discomfort based on SPSS

Model	R	R Square	Adjusted R Square	Independent Indicators due to table1	Dependent indicator	F	Sig.
1	.969	.938	.938	V.9		3764.2	.000
2	.975	.950	.950	V.9- V.1		2366.2	.000
3	.980	.961	.961	V.9- V.1- V.12		2021.7	.000
4	.985	.970	.969	V.9- V.1- V.12- V.11	Thermal Discomfort	1965.3	.000
5	.988	.977	.977	V.9- V.1- V.12- V.11- V.2		2083.3	.000
6	.989	.978	.978	V.9- V.1- V.12- V.11- V.2- V.10		1822.8	.000
7	.989	.979	.978	V.9- V.1- V.12- V.11- V.2- V.10- V.5		1587.3	.000

8	.989	.979	.978	V.9- V.1- V.12- V.11- V.2- V.10- V.5-V.6	1406.5	.000

Table 5. Tests of selected regression models of thermal discomfort based on SPSS

Model		B	Std. Error	T	Sig.
6	(Constant)	76.031	.160	475.271	.000
	Window ratio on south	-6.989	.071	-99.122	.000
	Length of class no. 1	-.186	.016	-11.667	.000
	Window ratio on west	-.551	.052	-10.608	.000
	Window ratio on north	-.715	.068	-10.534	.000
	Length of class no. 2	-.151	.017	-9.027	.000
	Window ratio on east	-.180	.050	-3.590	.000
8	(Constant)	76.475	.218	351.586	.000
	Window ratio on south	-7.010	.070	-100.279	.000
	Length of class no. 1	-.186	.016	-11.817	.000
	Window ratio on west	-.531	.052	-10.267	.000
	Window ratio on north	-.706	.067	-10.521	.000
	Length of class no. 2	-.151	.016	-9.154	.000
	Window ratio on east	-.165	.050	-3.319	.001
	Length of class no. 5	-.037	.016	-2.263	.025
	Length of class no. 6	-.032	.016	-1.996	.047

Table 7. Correlation diagrams of selected factors with thermal discomfort based on SPSS

Correlation of thermal discomfort and west window surface	Correlation of thermal discomfort and Length of class no. 1	Correlation of thermal discomfort and south window surface
Correlation of thermal discomfort and east window surface	Correlation of thermal discomfort and Length of class no.2	Correlation of thermal discomfort and north window surface
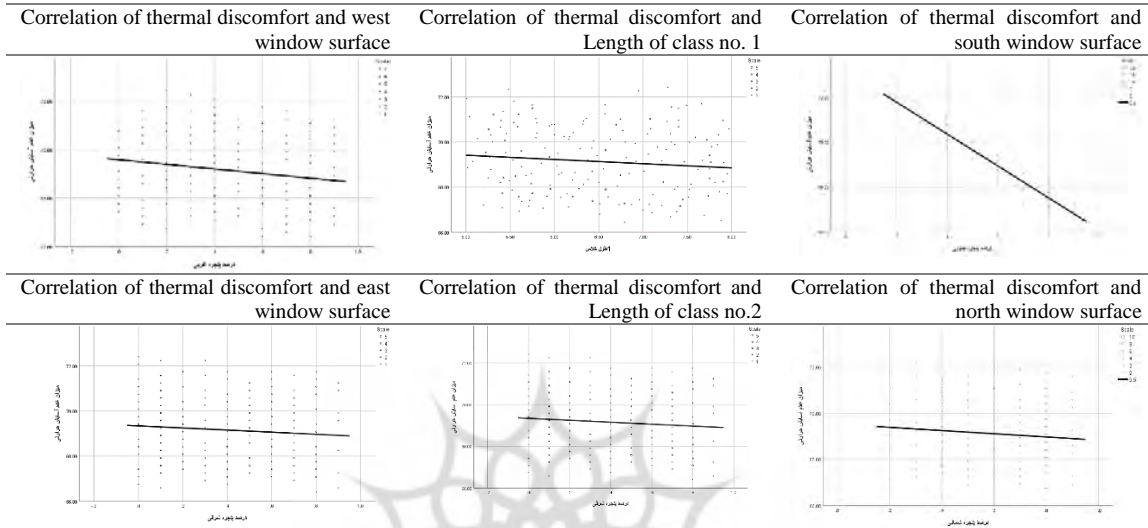
(2)

$$Y_{ThermalDiscomfort} = 76.031 - 6.989x_1 - 1.86x_2 - 0.551x_3 - 0.715x_4 - 0.15x_5 - 0.18x_6$$

Equation 2 can be used to summarize the findings of regression. In this equation, Y is thermal discomfort, and x1 to x6 represents the percentage of the south window area, class 1 length, west window area percentage, north window area percentage, class 2 length, and east window area percentage, respectively, whose coefficients are extracted from the B index of regression. Table 7 shows the regression diagram of each of the six factors of the model in relation to thermal discomfort.

The results indicate that the percentage of the openings, especially in the south, plays the most important role in thermal discomfort, and the design of the facade is more crucial than the plan. The second regression is related to the probability of glare in daylight. Regarding the visual comfort model according to Table 8, the first variable that is included in the equation is the percentage of the south

window area with a correlation coefficient of 0.574, which indicates a high relationship with the visual comfort of residents (Table 9).

The adjusted coefficient indicates that 32.7% of the visual discomfort is related to the ratio of the south window percentage. The second variable is the north window percentage, which adds another 30% to the adjustment coefficient by entering the model and acts as the second factor in visual comfort. East and west windows add about 10% to the model adjustment coefficient, respectively.

Class 1 and 2 lengths also accounted for nearly 3%, but their impact factor in Table 10 is small. Finally, the height of the north window is the last factor to enter the model.

Table 8. Details of stepwise regression models based on SPSS

model	Variables entered into the visual discomfort equation	Method
1	Window ratio on south	
2	Window ratio on north	
3	Window ratio on east	stepwise
4	Window ratio on west	
5	Length of class no. 1	
6	Length of class no. 2	
7	North window height	

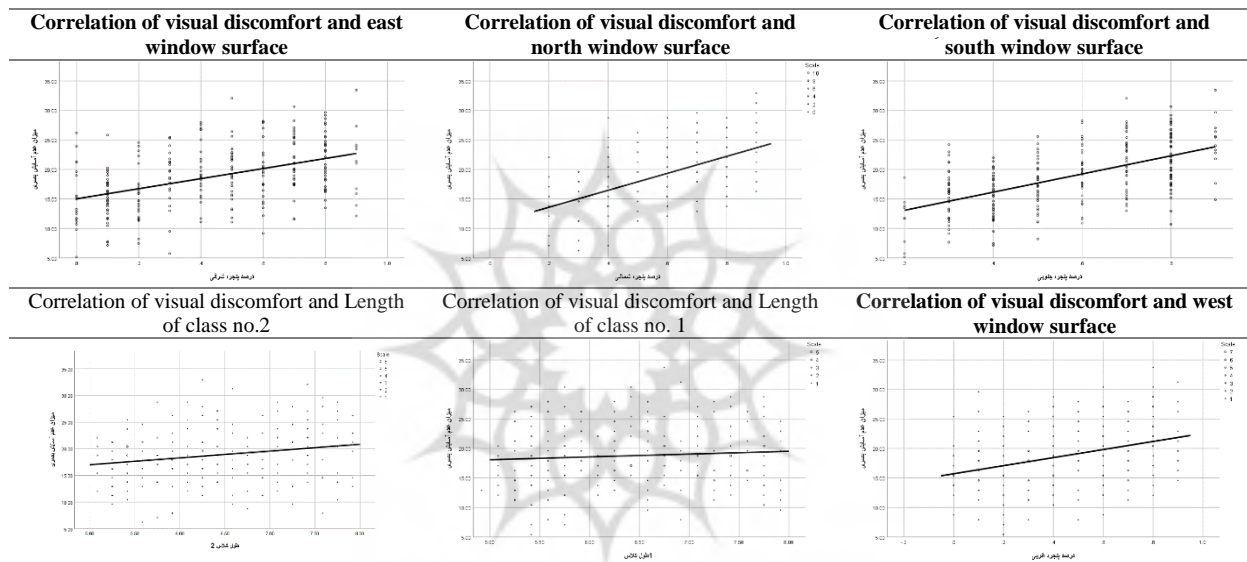Table 9. Details of the introduced regression models of visual discomfort based on SPSS

Model	R	R Square	Adjusted R Square	Independent Indicators due to table1	Dependent indicator	F	Sig.
1	.574	.329	.327	V.9		121.86	.000
2	.795	.632	.629	V.9- V.11		212.09	.000
3	.883	.779	.776	V.9- V.11- V.10	Visual Discomfort	289.07	.000
4	.935	.875	.873	V.9- V.11- V.10- V.12		429.15	.000

5	.951	.904	.902	V.9- V.11- V.10- V.12- V.2	461.60	.000
6	.956	.913	.911	V.9- V.11- V.10- V.12- V.2- V.1	425.70	.000
7	.960	.921	.919	V.9- V.11- V.10- V.12- V.2- V.1- V.8	403.65	.000

Table 6. Tests of selected regression models of visual discomfort based on SPSS

Model		B	Std. Error	T	Sig.
	(Constant)	-10.725	1.267	-8.466	.000
7	Window ratio on south	13.711	.491	27.944	.000
	Window ratio on north	14.339	.471	30.416	.000
	Window ratio on east	7.448	.349	21.331	.000
	Window ratio on west	6.000	.361	16.630	.000
	Length of class no. 2	1.032	.117	8.828	.000
	Length of class no. 1	.562	.111	5.078	.000
	North window height	-1.730	.350	-4.948	.000

Table 11. Correlation diagrams of selected factors with visual discomfort
based on SPSS

Correlation of visual discomfort and east window surface	**Correlation of visual discomfort and north window surface**	**Correlation of visual discomfort and south window surface**
Correlation of visual discomfort and Length of class no.2	Correlation of visual discomfort and Length of class no. 1	**Correlation of visual discomfort and west window surface**

(3)

$$Y_{VisualDiscomfort} = -10.725 + 13.711x_1 + 14.339x_2 + 7.448x_3 + 6x_4 + 1.032x_5 + 0.5628x_6 - 1.73x_7$$

By studying the correlation coefficients and B index, model 7 is the most appropriate model. And the formula for calculating the probability of glare from daylight is as follows. In this equation, x1 to x6 is equal to the area of the south, north, east, west window, class 2 length, class 1 length, and north window height, respectively. According to the proposed equation, visual discomfort is directly related to the percentage of opening in all four directions and the southern, northern, eastern, and western fronts are important, respectively. Due to their positive coefficient, the higher the opening

level, the higher the probability of glare is. In this regression, plan design factors are important only in the dimensions of two classes 1 and 2, which are located on the south side of the school but have a low coefficient. The last factor is the height of the window on the north front, which is proof that the higher the height of the window, the less glare. When it comes to visual comfort, the facade and the number of openings is crucial factors to consider. The last regression is related to the inappropriate carbon dioxide concentration equation. Table 12 shows the variables entered in the equation.

In the carbon dioxide concentration equation above 800 PPM, class 4, 2, and 5 lengths were entered into the model, which has a low correlation coefficient, and it can be concluded that the carbon dioxide concentration has not have a proven relationship with the 13 variables studied in this study (Table 13).

Table 12. Details of stepwise regression models of CO2 concentration based on SPSS

model	Variables entered into the CO2 concentration equation	Method
1	Length of class no. 4	stepwise
2	Length of class no. 2	
3	Length of class no. 5	

Table 13. Details of the introduced regression models of Co2 concentration based on SPSS

Model	R	R Square	Adjusted R Square	Independent Indicators due to table1	Dependent indicator	F	Sig.
1	.302	.091	.087	V.9	Co2 concentration	24.865	.000
2	.383	.147	.140	V.9- V.11		21.254	.000
3	.452	.204	.195	V.9- V.11- V.10		21.061	.000

4. Conclusion

The study framework began with the development of a generative algorithm that generated various floor designs based on defined criteria. Turning the plan into a zone, defining the opening regions and shading volumes, and then changing the materials completed the procedure. The simulation settings for thermal and visual comfort, as well as carbon dioxide concentration, have been finalized. To construct multiple models and save the simulation results, a random loop is established and performed 250 times. To explore the link between design elements and these three indicators, the simulation results by thermal and visual discomfort, as well as carbon dioxide concentration, are entered into a stepwise multivariate linear regression analysis. The regression findings demonstrate the importance of the school's southern front, both in terms of plan and façade elements. Visual and thermal comfort are connected to the window area on four distinct sides and the size of the southern classrooms, except for carbon dioxide concentration, which was not correlated with any of the thirteen criteria investigated. The comfort of the occupants is not affected by the proportions of the northern classrooms or the depth of the canopy. The thermal comfort in the classrooms improves as the window level rises, but the visual comfort declines. Also, due to the regression coefficients in the two equations of thermal and visual comfort, longer length in the southern classes has a favorable effect on thermal comfort, while its increase does not have a significant effect on glare. Therefore, by changing it while creating thermal comfort, visual discomfort can be avoided. There is a large gap between research on the technologies used in education and the impact this research has on middle schools (Mogas et al., 2021). One of the most significant successes of information technology development in terms of fundamentally changing the educational system is smart schools. Technology may be a strong instrument for

improving educational quality and efficiency, but it should be recognized that integrating information and communication technology into the education and learning system is a multidimensional and difficult process. Investment in school infrastructure and equipment should be enhanced, and the school should be regarded as a smart school from a holistic approach (Saini & Goel, 2019). Because school administrators have limited awareness of the potential and advantages of smart schools, smart education training programs, and professional development are required to aid them in the implementation process. To enhance individual and collective growth, smart classrooms should be supported with the development of life skills such as critical thinking, active engagement, and empowerment.

References

Alghamdi, S., Tang, W., Kanjanabootra, S., & Alterman, D. (2022). Effect of Architectural Building Design Parameters on Thermal Comfort and Energy Consumption in Higher Education Buildings. *Buildings, 12*(3), 329.

Asadi, I., Mahyuddin, N., & Shafigh, P. (2017). A review on indoor environmental quality (IEQ) and energy consumption in building based on occupant behavior. *Facilities*.

Bahaj, A. S., James, P. A., & Jentsch, M. F. (2008). Potential of emerging glazing technologies for highly glazed buildings in hot arid climates. *Energy and buildings, 40*(5), 720-731.

Buratti, C., Moretti, E., Belloni, E., & Cotana, F. (2013). Unsteady simulation of energy performance and thermal comfort in non-residential buildings. *Building and environment, 59*, 482-491.

Catalina, T., & Iordache, V. (2012). IEQ assessment on schools in the design stage. *Building and environment, 49*, 129-140.

Cetin, M. (2016). A Change in the Amount of CO2 at the Center of the Examination Halls: Case Study of Turkey. *Studies on Ethno-Medicine, 10*(2), 146-155.

Chaloeytoy, K., Ichinose, M., & Chien, S.-C. (2020). Determination of the Simplified Daylight Glare Probability (DGPs) Criteria for Daylit Office Spaces in Thailand. *Buildings, 10*(10), 180.

Choudhury, A. R., Majumdar, P., & Datta, C. (2011). Factors affecting comfort: human physiology and the role of clothing. In *Improving comfort in clothing* (pp. 3-60): Elsevier.

Comite'Europe'en de Normalisation, C. (2007). Indoor environmental input parameters for design and assessment of energy performance of buildings addressing indoor air quality, thermal environment, lighting and acoustics. *EN 15251.*

Diaz, M., Piderit, M. B., & Attia, S. (2021). *Parameters and indicators used in Indoor Environmental Quality (IEQ) studies: a review.* Paper presented at the Journal of Physics: Conference Series.

energy plus weather data. (2021).

Fisk, W. J. (2000). Review of health and productivity gains from better IEQ.

Fisk, W. J. (2002). How IEQ affects health, productivity. *ASHRAE journal, 44*(LBNL-51381).

Fisk, W. J., Black, D., & Brunner, G. (2011). Benefits and costs of improved IEQ in US offices. *Indoor Air, 21*(5), 357-367.

Handbook-Fundamentals, A., & Edition, S. (2009). Atlanta: American Society of Heating, Refrigerating and Air-Conditioning Engineers. *Inc.(see page 14.14 for summary description of RP-1171 work on uncertainty in design temperatures).*

Hollberg, A., & Ruth, J. (2016). LCA in architectural design—a parametric approach. *The International Journal of Life Cycle Assessment, 21*(7), 943-960.

Holzer, D., Hough, R., & Burry, M. (2007). Parametric design and structural optimisation for early design exploration. *International Journal of Architectural Computing, 5*(4), 625-643.

Jones, N. L. (2019). *The Imageless Method for Spatial and Annual Glare Analysis.*

Kabele, K., Veverková, Z., & Urban, M. (2019). *Methodology for assessing the indoor environmental quality in low energy buildings in the Czechia.* Paper presented at the IOP Conference Series: Materials Science and Engineering.

Kapalo, P., Vilcekova, S., & Voznyak, O. (2014). Using experimental measurements of the concentrations of carbon dioxide for determining the intensity of ventilation in the rooms. *Chemical Engineering Transactions, 39*, 1789-1794.

Karapetsis, A., & Alexandri, E. (2016). *Indoor Environmental Quality and its Impacts on Health–Case Study: School Buildings.* Paper presented at the Proceedings of the EinB2016—5th International Conference "ENERGY in BUILDINGS.

Lang, X., Wargocki, P., & Liu, W. (2022). Investigating the relation between electroencephalogram, thermal comfort, and cognitive performance in neutral to hot indoor environment. *Indoor Air, 32*(1), e12941.

Latha, P., Darshana, Y., & Venugopal, V. (2015). Role of building material in thermal comfort in tropical climates–A review. *Journal of Building Engineering, 3*, 104-113.

Lee, E. S., & Tavil, A. (2007). Energy and visual comfort performance of electrochromic windows with overhangs. *Building and environment, 42*(6), 2439-2449.

Lyons, P. R., Arasteh, D., & Huizenga, C. (2000). Window performance for human thermal comfort. *Transactions-American Society of Heating Refrigerating and Air Conditioning Engineers, 106*(1), 594-604.

Mazzeo, D., & Kontoleon, K. J. (2020). The role of inclination and orientation of different building roof typologies on indoor and outdoor environment thermal comfort in Italy and Greece. *Sustainable Cities and Society, 60*, 102111.

Middel, A., Selover, N., Hagen, B., & Chhetri, N. (2016). Impact of shade on outdoor thermal comfort—a seasonal field study in Tempe, Arizona. *International journal of biometeorology, 60*(12), 1849-1861.

Mogas, J., Palau, R., Fuentes, M., & Cebrián, G. (2021). Smart schools on the way: How school principals from Catalonia approach the future of education within the fourth industrial revolution. *Learning Environments Research*, 1-19.

Pereira, L. D., Lamas, F. B., & da Silva, M. G. (2019). Improving energy use in schools: from IEQ towards energy-efficient planning—method and in-field application to two case studies. *Energy Efficiency, 12*(5), 1253-1277.

Rahbar, M., Mahdavinejad, M., Markazi, A. H., & Bemanian, M. (2022). Architectural layout design through deep learning and agent-based modeling: A hybrid approach. *Journal of Building Engineering, 47*, 103822.

Razmi, A., Rahbar, M., & Bemanian, M. (2022). PCA-ANN integrated NSGA-III framework for dormitory building design optimization: Energy efficiency, daylight, and thermal comfort. *Applied Energy, 305*, 117828.

Renz, A., & Hilbig, R. (2020). Prerequisites for artificial intelligence in further education: identification of drivers, barriers, and business models of educational technology companies. *International Journal of Educational Technology in Higher Education, 17*(1), 1-21.

Saini, M. K., & Goel, N. (2019). How smart are smart classrooms? A review of smart classroom technologies. *ACM Computing Surveys (CSUR), 52*(6), 1-28.

Singh, M., Garg, S., & Jha, R. (2008). Different glazing systems and their impact on human thermal comfort—Indian scenario. *Building and environment, 43*(10), 1596-1602.

Suk, J. Y., Schiler, M., & Kensek, K. (2013). Development of new daylight glare analysis methodology using absolute glare factor and relative glare factor. *Energy and buildings, 64*, 113-122.

Tzempelikos, A., & Chan, Y.-C. (2016). Estimating detailed optical properties of window shades from basic available data and modeling implications on daylighting and visual comfort. *Energy and buildings, 126*, 396-407.

Wargocki, P., Wyon, D. P., Sundell, J., Clausen, G., & Fanger, P. O. (2000). The effects of outdoor air supply rate in an office on perceived air quality, sick building syndrome (SBS) symptoms and productivity. *Indoor Air, 10*(4), 222-236.

Wei, L., Tian, W., Zuo, J., Yang, Z.-Y., Liu, Y., & Yang, S. (2016). Effects of building form on energy use for buildings in cold climate regions. *Procedia Engineering, 146*, 182-189.

Wei, W., Wargocki, P., Zirngibl, J., Bendžalová, J., & Mandin, C. (2020). Review of parameters used to assess the quality of the indoor environment in Green Building certification schemes for offices and hotels. *Energy and buildings, 209*, 109683.

Wienold, J. (2007). *Dynamic simulation of blind control strategies for visual comfort and energy balance analysis.* Paper presented at the Building Simulation.

Wienold, J., & Christoffersen, J. (2005). Towards a new daylight glare rating. *Lux Europa, Berlin*, 157-161.

Wienold, J., & Christoffersen, J. (2006). Evaluation methods and development of a new glare prediction model for daylight environments with the use of CCD cameras. *Energy and buildings, 38*(7), 743-757.

Zhang, X., Weerasuriya, A. U., Wang, J., Li, C. Y., Chen, Z., Tse, K. T., & Hang, J. (2022). Cross-ventilation of a generic building with various configurations of external and internal openings. *Building and environment, 207*, 108447.